

Electronic Supplementary Information (ESI)

## Resolving the discrepancies in the reported optical absorption of low-dimensional non-toxic perovskites, Cs<sub>3</sub>Bi<sub>2</sub>Br<sub>9</sub> and Cs<sub>3</sub>BiBr<sub>6</sub>

Minh N. Tran,<sup>a</sup> Iver J. Cleveland,<sup>a</sup> Eray S. Aydil\*<sup>a</sup>

<sup>a</sup> Department of Chemical and Biomolecular Engineering, Tandon School of Engineering, New York University  
New York, New York 11201, United States

\*Corresponding author: ea2223@nyu.edu

### Film Thickness Determination

Optical absorptions of the films were recorded using an Agilent Cary 5000 UV-Vis-NIR in the 200-2000 nm range using a blank glass substrate as reference. Absorption was corrected for a small constant background such that all absorption remained positive in the entire 200-2000 nm range. Thin film interference fringes below the band gap energies were used to determine the film thicknesses using a two-layer model of a thin semitransparent absorbing film on a transparent substrate (glass). The incident light is non-polarized and the incidence is normal to the film and the substrate planes. Within this model the transmission is given by

$$T = \frac{8n_0n_1^2n_2}{(n_0^2+n_1^2)(n_1^2+n_2^2)+4n_0n_1^2n_2+(n_0^2-n_1^2)(n_1^2-n_2^2)\cos 2\delta_1} + T_o \quad [1]$$

where

$$\delta_1 = \frac{2\pi}{\lambda}n_1d_1\cos\varphi_1 \quad [2]$$

is the change in phase of the beam traversing the film,  $\lambda$  is the wavelength,  $d_1$  is the film thickness,  $\varphi_1$  is the angle of incidence (in this case, 90°), and  $n_0 = 1$ ,  $n_1(\lambda)$  and  $n_2 = 1.5$  are the refractive indices of air, the film, and the substrate, respectively.  $T_o$  is a wavelength independent shift that takes into account the reflections from the backside of the glass and any scattering.

The film thicknesses were determined by fitting the experimental data to equation 1 over a wavelength range where the sample does not absorb (i.e., light energies below the band gap energy of the respective films). The spacing between the successive local maxima and minima depends on the film thickness and the refractive index. Refractive index of CsBr was obtained from literature.<sup>1</sup> To our knowledge, refractive indexes of BiBr<sub>3</sub>, Cs<sub>3</sub>Bi<sub>2</sub>Br<sub>9</sub> and Cs<sub>3</sub>BiBr<sub>6</sub> have not been reported. We used two methods to extract the film thickness from the transmission data. First, we used the Swanepoel method.<sup>2</sup> Second, we used the two parameter Sellmeier equation

$$n^2 = 1 + \frac{B_1\lambda^2}{\lambda^2 - C_1} \quad [3]$$

to represent the refractive index and simultaneously fit the film thickness and the wavelength dependence of the refractive index. The fit thicknesses of Cs<sub>3</sub>Bi<sub>2</sub>Br<sub>9</sub> and Cs<sub>3</sub>BiBr<sub>6</sub> films was insensitive to the method and were within less than 2% of each other. Moreover, the Cs<sub>3</sub>Bi<sub>2</sub>Br<sub>9</sub> and Cs<sub>3</sub>BiBr<sub>6</sub> film thicknesses determined from these fits are within 2% of the values calculated using the deposition rates from

$$R_i = R_{CsBr} \frac{1}{3} \frac{M_i}{M_{CsBr}} \frac{\rho_{CsBr}}{\rho_i} \quad [4]$$

where  $R_i$  and  $R_{CsBr}$  are the deposition rates of the products ( $i = \text{Cs}_3\text{Bi}_2\text{Br}_9$  or  $\text{Cs}_3\text{BiBr}_6$ ) and CsBr, respectively. The experimental fits to the transmission are shown for all four materials in Figure S1 (a)-(d) and the corresponding thicknesses are in the Figure captions. The refractive indices fit using equations 1 and 3 are shown in Figure S1(e). All depositions were 1800 s and the tooling factors determined from these measurements were 39.7 and 42.9 for CsBr and BiBr<sub>3</sub>, respectively.

$$TF = \frac{\text{Deposition Rate on the Substrate}}{\text{Deposition rate on QCM}}$$

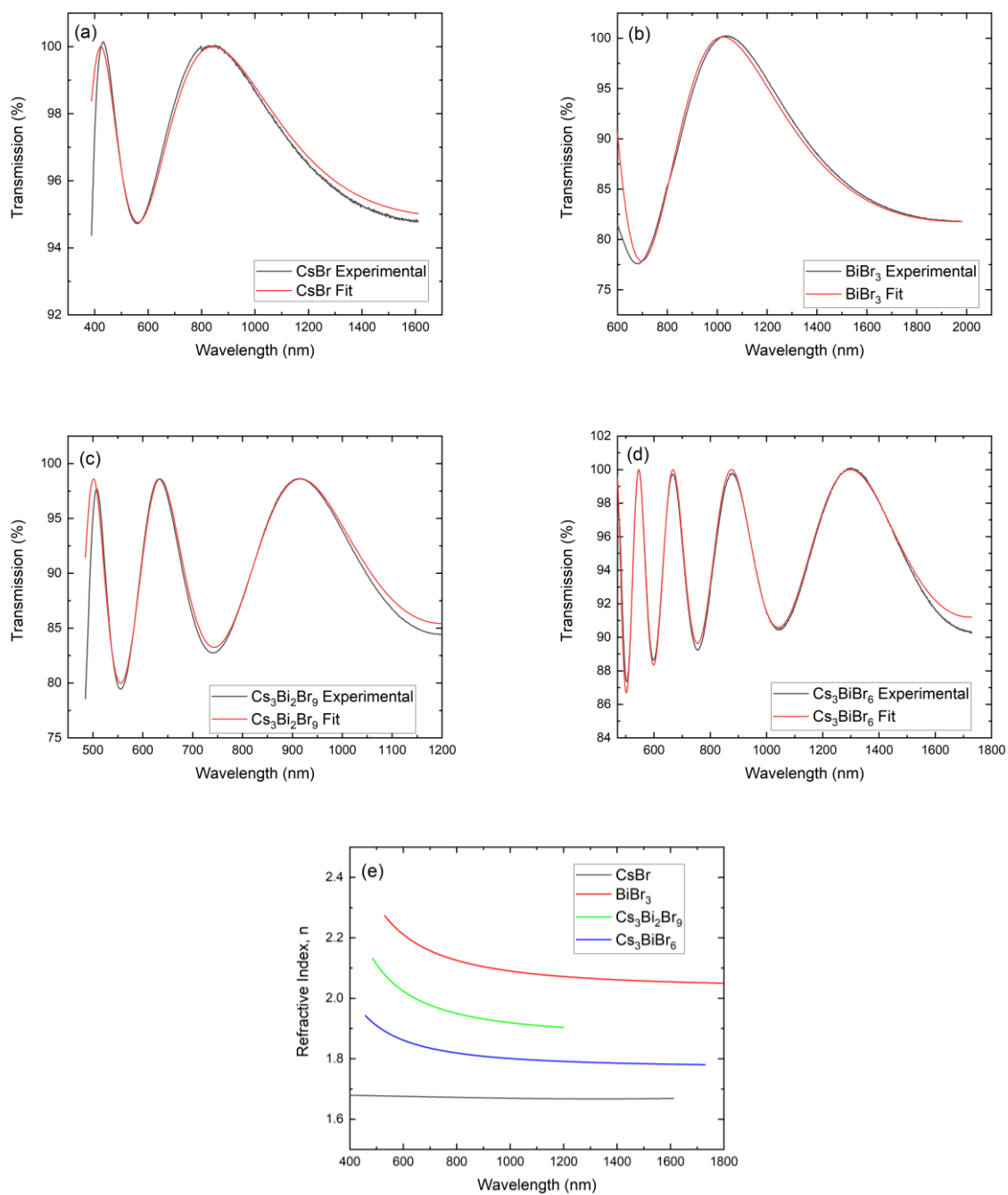


**Figure S1.** Typical experimental transmission curves and fits using film thicknesses of (a) CsBr (252 nm), (b) BiBr<sub>3</sub> (245 nm), (c) Cs<sub>3</sub>Bi<sub>2</sub>Br<sub>9</sub> (475 nm) and (d) Cs<sub>3</sub>BiBr<sub>6</sub> (727 nm) for this particular set of films. (e) The refractive indices extracted for BiBr<sub>3</sub>, Cs<sub>3</sub>Bi<sub>2</sub>Br<sub>9</sub>, and Cs<sub>3</sub>BiBr<sub>6</sub>; the CsBr refractive index is from reference 1.

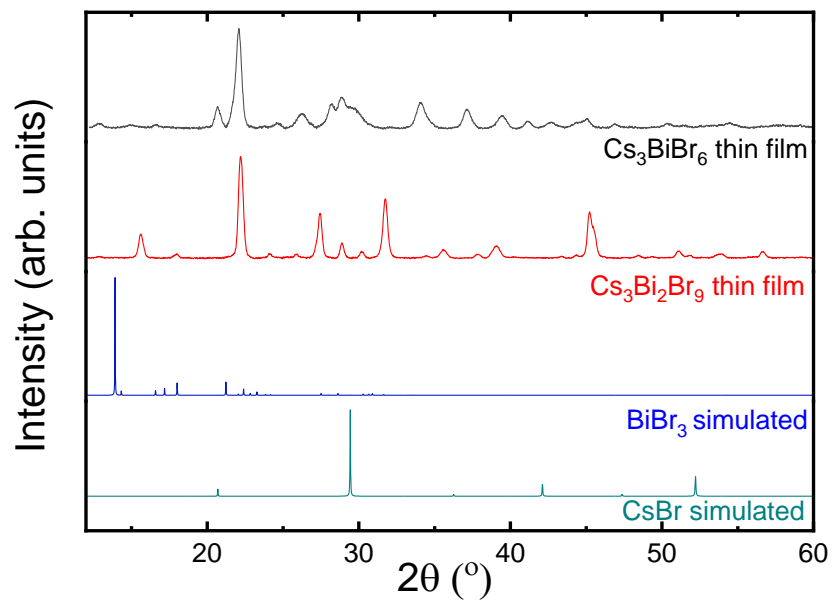


**Figure S2.** A comparison of the XRD patterns from as-deposited Cs<sub>3</sub>Bi<sub>2</sub>Br<sub>9</sub> and Cs<sub>3</sub>BiBr<sub>6</sub> thin films and the two precursors CsBr and BiBr<sub>3</sub>. The Cs<sub>3</sub>Bi<sub>2</sub>Br<sub>9</sub> and Cs<sub>3</sub>BiBr<sub>6</sub> thin films do not show the major diffraction peaks from the precursors indicating that CsBr and BiBr<sub>3</sub> have reacted completely and are absent from the films within the detection limits of XRD.

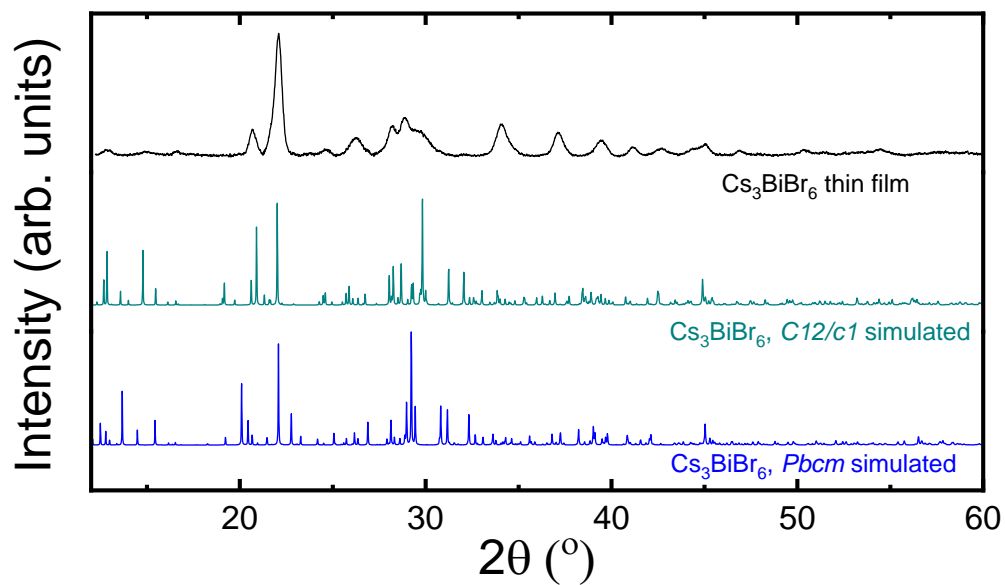


**Figure S3.** XRD patterns of Cs<sub>3</sub>BiBr<sub>6</sub> thin film deposited by PVD and the simulated XRD patterns of the structures reported by Tang *et al.* (*Pbcm*, #57 from single crystals) and Yang *et al.* (*C12/c1*, #15, nanocrystals).

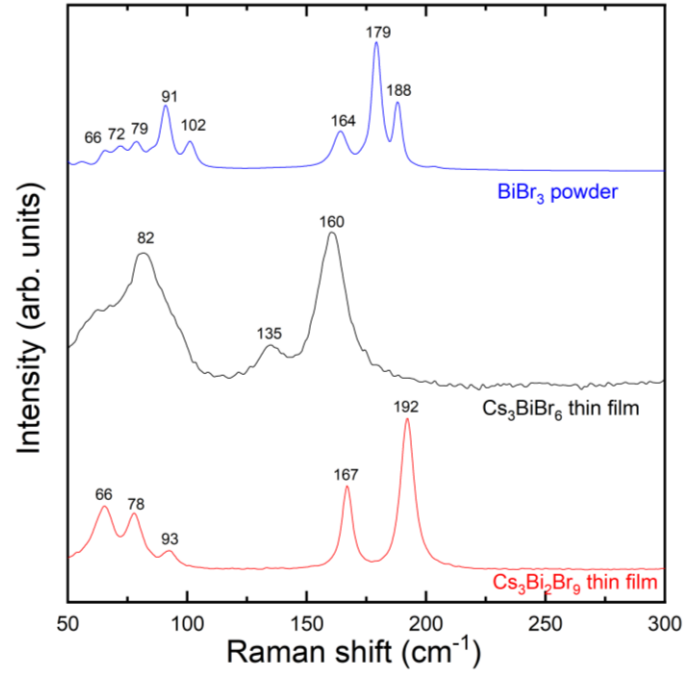


**Figure S4.** Raman spectra of Cs<sub>3</sub>Bi<sub>2</sub>Br<sub>9</sub>, Cs<sub>3</sub>BiBr<sub>6</sub> thin films and BiBr<sub>3</sub> powder.

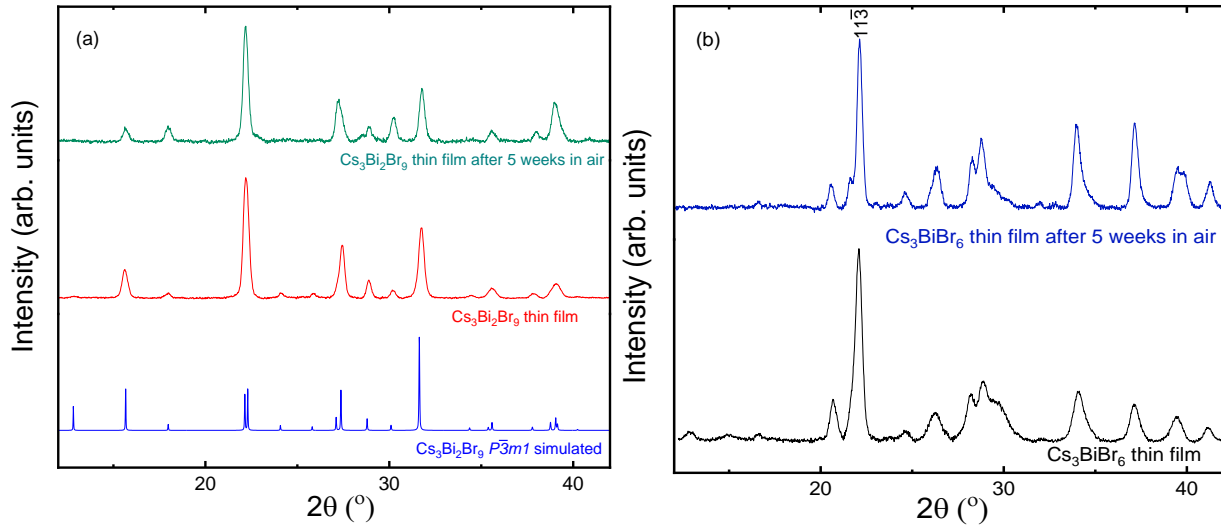


**Figure S5.** XRD patterns of as deposited (a) Cs<sub>3</sub>Bi<sub>2</sub>Br<sub>9</sub> and (b) Cs<sub>3</sub>BiBr<sub>6</sub> thin films and the same films after 5 weeks. Cs<sub>3</sub>BiBr<sub>6</sub> peak widths decreased after 5 weeks indicating grain growth even at room temperature. Average grain sizes calculated from the 11 $\bar{3}$  XRD peak at  $22^\circ$  using Scherrer equation increases from 17 nm to 24 nm.

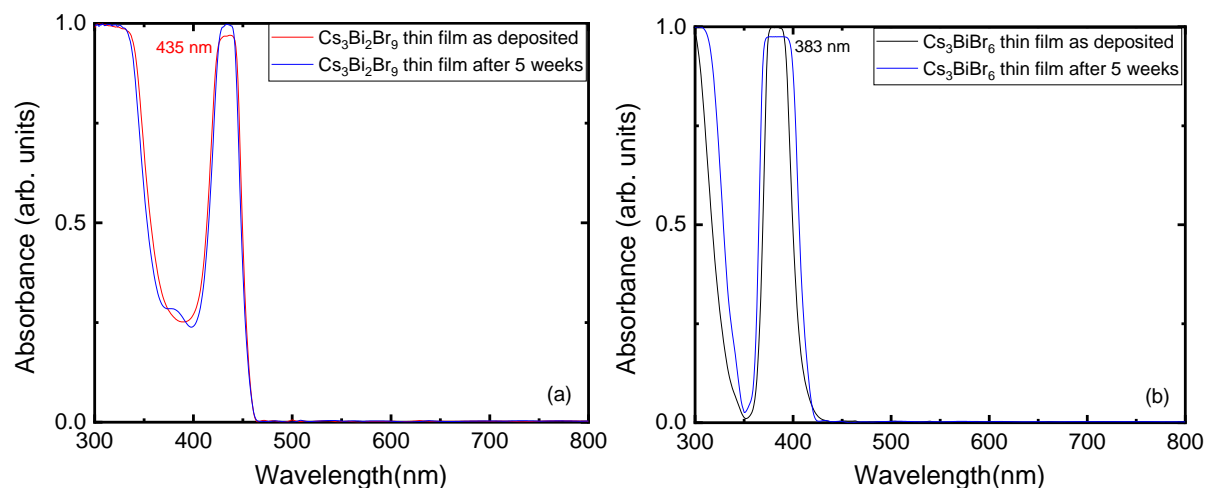


**Figure S6.** Comparison of the absorption spectra of (a)  $\text{Cs}_3\text{Bi}_2\text{Br}_9$  and (b)  $\text{Cs}_3\text{BiBr}_6$  films after deposition and after 5 weeks in air.

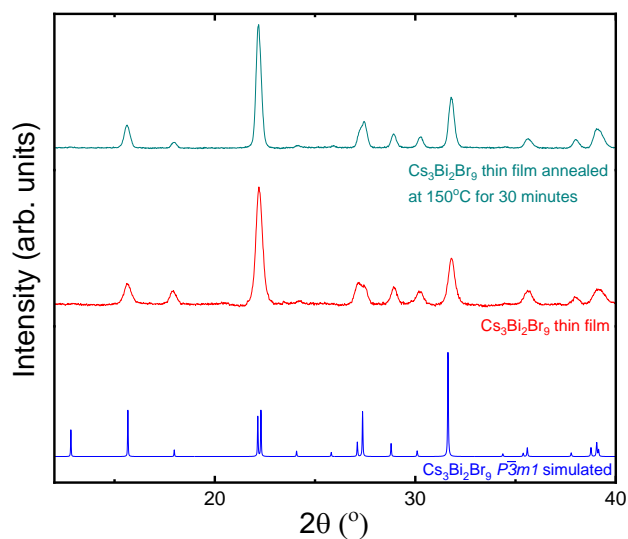


**Figure S7.** XRD patterns of  $\text{Cs}_3\text{Bi}_2\text{Br}_9$  thin film before and after annealing at  $150^\circ\text{C}$  for 30 minutes.

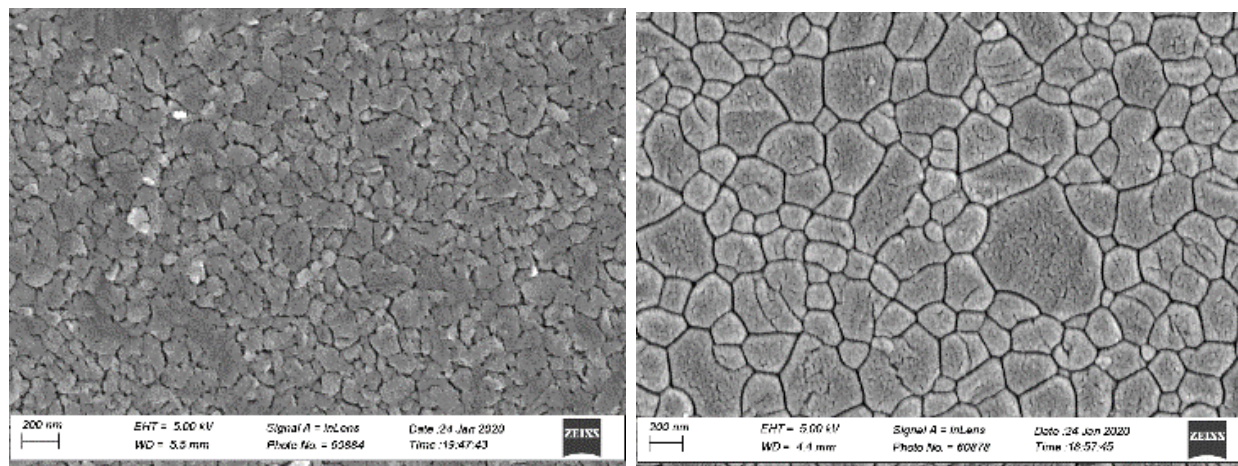


**Figure S8.**  $\text{Cs}_3\text{Bi}_2\text{Br}_9$  before and after annealing at  $150^\circ\text{C}$  for 30 minutes.

### Exciton Bohr radius Estimation

Exciton Bohr radius is given by

$$a_{ex} = \varepsilon_r \frac{m_o}{\mu_r} a_B , \quad [5]$$

where  $\varepsilon_r$  is the static relative permittivity ( $\varepsilon_r \sim 4$ ),  $m_o$  is the mass of an electron,  $a_B=0.053$  nm is the Hydrogen Bohr Radius and  $\mu_r$  is the reduced mass, given by

$$\mu_r = \frac{m_e m_h}{m_e + m_h} . \quad [6]$$

Taking  $m_e = 0.539 m_o$  and  $m_h = 2.279 m_o$  from reference 3 (accessed April 20, 2020) we obtain  $a_{ex} \approx 0.5$  nm. The unit cell dimensions for  $\text{Cs}_3\text{Bi}_2\text{Br}_9$  in the calculations reported in reference 3 are slightly different than those measured experimentally but this difference will have only a small effect on the estimate. The important conclusion is the exciton radius in  $\text{Cs}_3\text{Bi}_2\text{Br}_9$  is on the order of or smaller than the unit cell dimensions, about the size of a  $(\text{BiBr}_6)^{3-}$  octahedral.

---

<sup>1</sup> H. H. Li. *J. Phys. Chem. Ref. Data.*, 1976, **5**, 329-528.

<sup>2</sup> R. Swanepoel. *J. Phys. E: Sci. Instrum.*, 1983, **16**, 1214-1222.

<sup>3</sup> K. Persson. *Materials Project*, 2014, <https://materialsproject.org/docs/calculations> <https://dx.doi.org/10.17188/1201787>